Analysis of Space Charge Generating Devices for Lightning Protection: Performance in Slow Varying Fields

Farouk A. M. Rizk, *Life Fellow, IEEE*

***Abstract*—This paper starts with a review of anode corona modes with particularly streamer-free glow known as ultra-corona, with the view of exploring its application in lightning protection. Due to the inherent intensification of the ambient electric field atop a tall structure, strict conditions have to be imposed on the streamer-free space charge generation and the stability of that mode of corona when exposed to rapid field variations due to remote lightning. A novel ultra-corona electrode satisfying the above conditions is introduced. High voltage test results on such electrodes are presented including corona current, charge and laboratory air gap breakdown voltage. By applying dimensional analysis, a generalized formula for corona currents from such a device atop a tall structure is presented which includes the effects of the ambient ground field, structure height, ambient electric field at the top of the structure, electrode dimensions, and wind speed.**

***Index Terms*—Leader, lightning, space charge, streamers, ultra-corona.**

I. Introduction

PRESENT day lightning protection technology is mostly based upon the application of Franklin rods or overhead ground wires [1]. They act as preferential striking sites and, with proper grounding system, transfer the lightning stroke current safely to earth. This conventional technology has the advantage of simplicity and, at least for the Franklin rod, is generally inexpensive. A legitimate question is then why would anybody look for an alternative lightning protection technology which would likely be more complex and probably more expensive?

The justification for the search for a viable alternative lightning protection technology for both upward and downward flashes may be found in the following list.

1) Due to ambient ground field preceding a downward stepped leader, and particularly with tall structures, the Franklin rod may produce sufficient space charge (corona) as to self-protect. This allows the structure to be hit on the side rather than at the top. It may also allow strikes within the assigned protection zone [2].
2) Conventional ground wires as a means of lightning protection are far from perfect. Power engineers are quite familiar with shielding failures and backflashovers.
3) With modern power quality requirements there is an incentive to reduce the number of lightning strikes.
4) Even with successful single pole switching (auto-re-closure) there is an incentive to minimize the number of lightning faults with associated power-follow currents in order to reduce the wear and tear of switchgear.
5) Repeated lightning strikes, even when they do not produce overvoltages exceeding the substation protective level, constitute an unwelcome stress to power transformer and shunt reactor windings.
6) Limitations of present lightning protection technology by ground wires led sometimes to the application of transmission line arresters.
7) Lightning receptors on a wind turbine blade, which essentially act as Franklin rods, sometimes fail to intercept the lightning strike with consequent damage and expensive repairs [3].
8) Even when the lightning receptors on a wind turbine blade act as Franklin rods as intended, the stroke current which flows through the main mechanical bearing can cause significant damage [3]

Manuscript received November 14, 2008; revised June 02, 2009. First published April 05, 2010; current version published June 23, 2010. Paper no. TPWRD-00855-2008.

The authors is with the Expodev, Inc. and Lightning Electrotechnologies Inc., Montreal, QC J4S 1W2, Canada.

Digital Object Identifier 10.1109/TPWRD.2010.2044423

II. Review of Previous Work

It is generally appreciated that the presence and movement of space charge play a major role in lightning discharge formation and propagation. Space charges ahead of the descending leader tip significantly contribute to such fundamental phenomena as branching and formation of leader steps as well as pauses between steps [1].

The more favorable experience with blunt Franklin rods as compared to sharp rods [4] can be understood by some shielding effect from the space charge generated in the vicinity of the sharp tip due to the ambient ground field preceding a downward leader.

Before analyzing the effects of space charge due to coronas from different electrodes on lightning protection it is important to consider the different modes of corona discharges. Since the presence of a critical streamer [5] is a prerequisite for leader formation [6], special attention will be paid to space charge generation in the glow mode (i.e., streamer-free space charge generation).

Uhlig [7] experimentally investigated corona modes from fine point and thin wire electrodes. Two basic corona modes were identified; a streamer mode and a streamerless glow that was coined "ultra-corona". In the case of fine points, streamer discharges did not originate from the very tip but from the stem.

However in the case of thin wires only the streamer-free ultra-corona was encountered. Uhlig concluded that the ultra-corona requires high surface field stress with large perpendicular variation but zero tangential variation. Such conditions for ultra-corona are met by the field stresses produced by the elongated, longitudinal section formed between the two termini of a very thin wire. Streamers however are developed with lower surface stress and small variations in this stress in both the perpendicular and tangential directions, these conditions are satisfied by the stem of a sharp point or the top of a blunt point.

For air gaps with such thin wire electrodes no streamers formed from the thin wire right up to breakdown [7]. In tests with alternating and direct voltages on thin wire-ground plane gaps, a substantial increase in the mean breakdown gradient was achieved compared to a conventional rod-plane gap in the 100 cm range. Uhlig concluded therefore [7] that the ideal electrode shape fulfilling the requirements for ultra corona is the thin wire (not points).

In a test series with positive impulses Uhlig determined [7] that there is a critical rate of rise of the impulse voltage applied to the thin wire above which a significant deterioration of the short air gap (2 cm–12 cm) breakdown voltage takes place. It is noteworthy that the critical rate of voltage rise increased from roughly $0.1\ \mathrm{kV}/\mu\mathrm{s}$ for a 1mm diameter wire, to $1.0\ \mathrm{kV}/\mu\mathrm{s}$ for a 0.1 mm diameter wire. This demonstrates at least qualitatively the beneficial effects of thin wires on ultra-corona stability

Popkov [8] reported on HVDC transmission line investigation of the radio interference characteristics of a positive ACSR 280/300 3-conductor bundle mounted 2.6 meters above ground plane. In one test configuration, the conductor was provided with a spiral wire of 2 mm diameter with a spiral pitch of 50 mm, under dry conditions. It was found that, within a wide conductor gradient range the application of the relatively thin wire spiral substantially reduces the radio interference level by affecting the corona mode from streamer to glow. It was mentioned that this has been associated with greater corona losses (and evidently space charge) thereby discouraging this application on long transmission lines.

Reference [9] reports on ac tests carried out at Hydro-Quebec Research Institute (IREQ) by Heroux to investigate means for improving HV conductor corona performance, particularly for audible noise. The tests confirmed that production of ionic space charge by corona lowers the electric field at the conductor surface, tending to suppress corona activity. When enough ions are produced by pulseless glow, little electromagnetic interference was experienced. One ion-shielded conductor was realized by applying a very thin stainless steel fiber, manufactured under the name Bekinox, to the conductor surface. In tests with conductors wrapped with a so-called Bekitex fabric, woven from polyamide and Bekinox fiber containing 25% stainless steel fiber, streamers were suppressed entirely within a wide range of conductor surface gradients. This resulted in a substantial improvement in audible noise but here again the substantially increased rate of space charge production led to increased corona losses as reported previously by Popkov [8] for dc conductors.

A systematic study of modes of corona discharges in air has been reported by Giao Trinh and J.B Jordan [10].

Of particular interest to the present investigation are corona modes from a positive cylindrical conductor (anode corona). With spherical and conical protrusions Trinh and Jordan [10] reported on different modes of corona in a given air gap as the voltage is raised to breakdown. For the conical protrusion (points) the discharges started with onset streamers followed by positive glow, then a combination of streamers and positive glow as pre-breakdown streamers are approached. This demonstrates that sharp points on a tall structure exposed to a practical range of ambient field conditions can not be expected to produce only streamer-free corona.

There is a long history of attempts to use space charge effects in lightning protection. Golde [11] critically reviewed developments based upon the use of multiple points to neutralize cloud charges. The thrust of Golde's review is that charges due to corona produced by multiple points are far too small to have any significant effects on cloud charges. On the practical side Golde [11] noted that large forests which constitute millions of discharge points have obviously not been effective in discharging or neutralizing a thunder cloud passing over.

A different explanation of the mode of operation of a space charge system based upon multiple-point electrode (Dissipation Array) was put forward by Carpenter and Auer [12]. It was mentioned that the space charge from the ionizer (the multiple points) would neutralize the positive charge on the ground that would otherwise accompany the negative cloud charge overhead. This was criticized by Uman and Rakov [13] on the basis of a lack of quantitative arguments. Uman and Rakov [13] also disputed the notion contained in an IEEE Draft (IEEE P1576/D2.01(2001)) that a sufficient number of array points could emit a charge equal to that of a stepped leader (apparently taken as 5 C) in a cloud charge regeneration time of typically 10 s.

In a more recent publication [14], it is theorized that a multi-point electrode produces no more corona charge than an ordinary rod. Still it was suggested that the advantage of the multi-point electrodes lies in the division of corona current equally among the numerous points. This would delay or prevent streamer formation by maintaining the current in each individual point below a critical value supposedly needed for streamer formation. Although the notion of division of corona current among several needles on a large electrode (not necessarily equally) has been tentatively proposed by Golde [11] 30 years ago, this concept has not been verified either by laboratory experiment or in the field. Since in addition to the statistical nature of initiatory electrons, field conditions are bound to involve wind, rain, pollution and corrosion of the electrode points, both the notion of the division of the corona current equally among a multitude of points and the existence of a critical corona current for streamer formation lack validation under realistic conditions.

A critical paper of the so-called lightning elimination devices (including dissipation arrays or charge transfer systems) has been published by Mousa [15]. Any improvement in the upward flash lightning performance of tall structures (above 300 m effective height, that is, including altitude) was attributed to geometrical factors rather than to space charge effects (increasing the effective radius of the tower top). It is known however that

geometrical effects are generally ineffective under rain and are only effective under dry clean conditions. Secondly Mousa argued that such improvements, if true, do not apply to power lines or substations since, due to their limited heights, they do not normally experience upward flashes.

A simplified mathematical analysis of the effect of corona space charge on leader initiation under thunderstorm conditions is given by Aleksandrov *et al.* [16]. The paper comprises a mathematical model of a streamer-free corona discharge (ultra corona) occurring on a grounded spherical electrode of small radius (e.g., 5 cm) in free space. The model is based upon a quasi-steady simultaneous solution of the charge continuity and Poisson's equations as function of time in spherical coordinates in free space, neglecting the effect of the ground connection (support) on field distribution. The ambient ground field and accordingly the space potential of the spherical electrode in free space was mostly assumed to increase linearly with time in typically 10 s duration of cloud charge regeneration time.

Due to electric field reduction Aleksandrov *et al.* [16] conclude that space charge hinders initiation and development of an upward streamer/leader from the top of a high grounded object so that the effect strongly reduces the frequency of the appearance of upward lightning under thunderstorm conditions.

The authors suggested several topics of future work [16]. Of particular interest are suggestions as follows.

1) To study the conditions for leader initiation near electrodes of different shapes, with the purpose of estimating the possibilities for using corona effects for practical lightning protection. This point is particularly important since their paper, being basically theoretical, assumed ultra-corona generation from the spherical electrode without suggesting practical means to achieve that end. This constitutes one of the objectives of this paper.
2) To investigate the effect of a fast changing electric field due to a distant downward lightning leader on the corona and leader process. This point which constitutes the basic criticism of the Aleksandrov *et al.* paper by Uman and Rakov [13] is addressed below but transients due to negative leader decent will be investigated in a future publication.

The problem of nonstationary corona from rod electrodes has also been studied under simplified assumptions in more recent publications by Aleksandrov *et al.* [17], [18]. The basic model however remains that of the solitary sphere elaborated in more detail in [16]. Despite its merits, the modeling work of Aleksandrov suffers from some limitations which are bound to restrict general acceptance of its conclusions for practical applications as follows.

- It assumes only ultra-corona production without due consideration of the different modes of corona such as onset streamers, a mixture of glow and streamers, etc. [10], in the practical range of ambient electric fields to which the stressed point is exposed.
- It does not rigorously account for the effect of the field intensification at the structure top.
- It does not account for the effect of the ambient field at the space charge cloud boundary.
- It ignores the effect of water droplets due to rain, which are bound to exist on the otherwise assumed smooth surface of the spherical electrode and its effects on local field intensification and streamer formation.
- It ignores the effects of wind speed on corona current for various structure heights and different values of the ambient ground field.

Fortunately, the point discharge has been extensively investigated by meteorologists both in the laboratory and in the field [19]–[21], providing a wealth of data to compare with the predictions of the model of [16]. Whipple and Scrase [19] measured the corona discharge current from a point 8.4 meters above ground, exposed to natural fields due to cloud charges. It was confirmed that the dependence of the corona current on ambient ground fields in the range 1–16 kV/m follows a quadratic law, in agreement with laboratory measurements of stationary corona. This is in contrast to the model of Aleksandrov *et al.* [17] which predicts different laws governing corona from grounded structures under cloud charges and laboratory gaps.

Davis and Standring [20] investigated corona currents associated with kite balloons. In thundery weather the balloon was usually flown at 600 m. The results showed sustained balloon cable currents of several milliamperes flowing for minutes involving charges of the order of a coulomb. In one measurement corona currents as high as $-17\ \mathrm{mA}$ and $+25\ \mathrm{mA}$ have been recorded with associated durations of approximately 10 minutes and 3.5 minutes, respectively. In an attempt to explain the discharge mechanism the authors attributed initial upward discharges to electric fields at the earthed electrode sufficient to cause ionization by electron collision. The higher the electric field the longer is the avalanche path and the greater the probability of streamer formation [20]. Even with due consideration to the 600 m height, the recorded currents in the tens of milliampere range and particularly the duration of the sustained current flow can not be accounted for by the model of Aleksandrov *et al.* [16].

Large and Pierce [21] experimentally investigated the effect of wind speed on corona current from a positive point electrode installed 4 m above ground in open space. The discharge current was measured under an applied voltage corresponding to a mean electric field in the range of 9–15 kV/m. Large and Pierce found considerable influence of wind speed on the corona discharge current [21], a factor ignored in the model of Aleksandrov *et al.* [16]–[18].

The following empirical formula was obtained in [21] relating the sustained corona current i to the applied voltage V, corona inception voltage V_{ci}, and wind speed V_w:

$$i = A(V - V_{ci}) \cdot \sqrt{c^2 V^2 + V_w^2} \tag{1}$$

where, for a constant height of the point electrode above ground, and A and c are constants.

III. Field Intensification

In practical situations an ultra-corona device will be placed atop a tall structure where the field E_t is necessarily far more intense than the ambient ground field E_g. Since corona current is

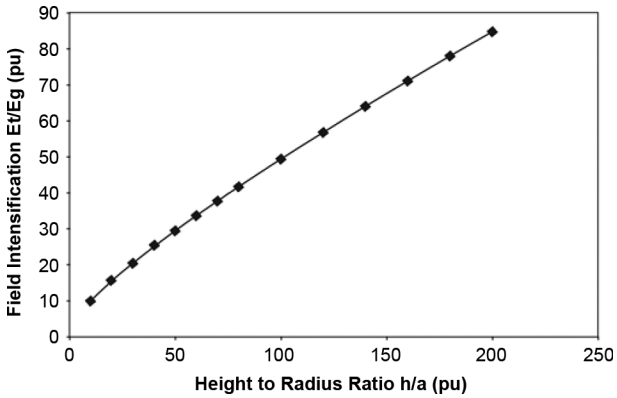

Fig. 1. Field intensification at semi-ellipsoid structure top.

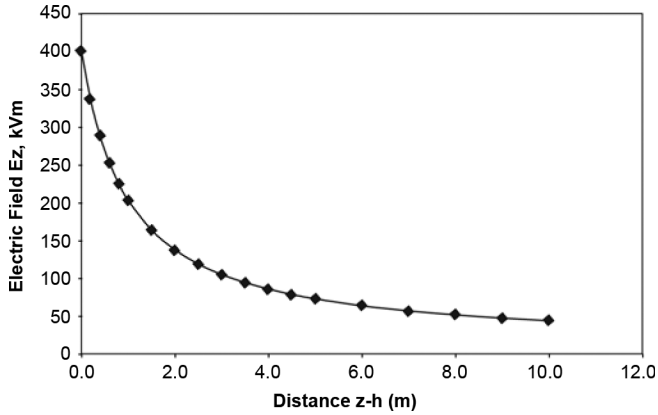

Fig. 2. Variation of axial electric field above structure top, $h = 150\,\mathrm{m}$, $h/a = 75$, $Eg = 10\ \mathrm{kV/m}$.

determined by the rate of removal of space charge from the electrode vicinity, this field intensification will have a determining effect on the current. The field intensification ratio E_t/E_g is presented in Fig. 1 as a function of the ratio h/a of the structure height "h" to the radius of curvature "a" at the top, for a semi-ellipsoid structure. It is shown that for $h/a = 50$, the field intensification ratio $E_t/E_g \approx 30$, so that for a ground field E_g of 10 kV/m, the field E_t at the top will be approximately 300 kV/m. Fig. 2 shows the variation of the axial field above the top of a structure with $h = 150\,\mathrm{m}$ and $a = 2\,\mathrm{m}$, for $E_g = 10\ \mathrm{kV/m}$. It is shown that the field starts at approximately 400 kV/m at the tower top and drops to 105 kV/m over a distance of 3 m. This shows that under these conditions once a streamer is initiated at the tower top it could reach lengths in the meter range [22]. This underlines the necessity of using an ultra-corona electrode with stable glow mode corona over a wide range of space potentials.

IV. Ultra-Corona Generating Devices

A. Critical Rates of Voltage Rise

In general successful application of ultra-corona devices for lightning protection depends on the stability of the ultra-corona under high rates of voltage (space potential) rise associated with descending negative leaders. This factor is more critical for protection against downward flashes and will therefore be dealt with further in a future publication.

In [2] it was argued that for stability of ultra-corona, a voltage increase at rate A in an infinitesimal interval Δt, must be able to generate enough positive ions which can move away from the electrode within that time interval so that the maximum field does not exceed the corona inception field E_{ci}. Using the charges on a sphere due to the applied voltage (space potential) and those induced due to space charge, it was determined that to maintain ultra-corona on a spherical electrode, the rate of voltage rise should satisfy the condition

$$A = \frac{dV}{dt} \leq 2\,\mu E_{ci}^2 \tag{2}$$

where μ is the positive ion mobility, taken as $2\times10^{-4}\,\mathrm{m^2/V\cdot s}$. A slightly different approach is described in the following: For a sphere of radius r at the corona inception voltage

$$\frac{V}{r} = E_{ci}. \tag{3}$$

The voltage rise during an interval Δt is

$$\Delta V = A \cdot \Delta t. \tag{4}$$

During that time interval the space charge moves by

$$\Delta r = \mu E_{ci} \Delta t. \tag{5}$$

The condition for maintaining ultra-corona is that the field at the new boundary $r + \Delta r$ must not exceed E_{ci}. At the boundary

$$\frac{V + \Delta V - E_{ci}\Delta r}{r + \Delta r} \leq E_{ci} \tag{6}$$

which yields

$$\Delta V \leq 2E_{ci}\Delta r. \tag{7}$$

Substituting for ΔV and Δr from (4) and (5)

$$A \cdot \Delta t \leq 2E_{ci} \cdot \mu E_{ci} \Delta t$$

or

$$A \leq 2\,\mu E_{ci}^2 \tag{8}$$

which is identical to (2) and confirms the present approach which is now going to be used for the case of a cylindrical conductor.

Consider a cylindrical conductor of radius r at height h above ground assumed to be in ultra corona. At corona inception

$$\frac{V}{r \ln \frac{2h}{r}} = E_{ci} \tag{9}$$

again

$$\Delta V = A \cdot \Delta t \tag{10}$$

and

$$\Delta r = \mu E_{ci} \Delta t. \tag{11}$$

The electric field at the new boundary $r + \Delta r$ must not exceed E_{ci} if ultra-corona is to be maintained. This means

$$\frac{V + \Delta V - E_{ci}\Delta r}{(r + \Delta r)\ln \frac{2h}{(r+\Delta r)}} \leq E_{ci} \tag{12}$$

which results in

$$\Delta V \leq \ln \frac{2h}{r} \cdot \Delta r \cdot E_{ci}. \tag{13}$$

Substituting for ΔV and Δr from (10) and (11), the stability criterion for ultra-corona in cylindrical geometry becomes

$$A \leq \mu \cdot \ln \frac{2h}{r} \cdot E_{ci}^2. \tag{14}$$

Noting that for large heights above ground $\ln 2h/r \gg 1$, comparing (14) and (8) shows that the critical rate of voltage rise for a cylindrical conductor is several times higher than that of a sphere (point) electrode even at the same critical gradient E_{ci}. This property is fundamental in preventing ultra-corona instability due to rapidly varying fields and tends to support the potential application of ultra corona generating conductors for lightning protection.

When using very thin wires E_{ci} will be higher and the critical rate of voltage rise can be brought into a range of practical interest, something that can not be practically achieved with a sphere (point electrode).

It is of interest to apply this approach to estimate the critical rate of voltage for a toroidal electrode assumed to be in ultra-corona mode. It is well known that toroidal electrodes are widely used on high voltage insulators and power apparatus. Consider a toroid with a major radius b, minor radius replaced at a height h above ground. Let $b \gg r$ and $h \gg b$. The basic equations for estimating the critical rate of voltage rise are

$$\frac{V}{rG\left(\frac{r}{b}\right)} = E_{ci} \tag{15}$$

with

$$G\left(\frac{r}{b}\right) = K\left(m, \frac{\pi}{2}\right) \tag{16}$$

where K is the complete elliptic integral of the first kind and $m^2 = 1 - (r/2b)^2$

$$\Delta V = A \cdot \Delta t \tag{17}$$

$$\Delta r = \mu E_{ci} \cdot \Delta t. \tag{18}$$

At the new boundary $r + \Delta r$, the required condition for stability of ultra-corona is written as

$$\frac{V + \Delta V - E_{ci}\Delta r}{(r + \Delta r)G\left(\frac{(r+\Delta r)}{b}\right)} \leq E_{ci} \tag{19}$$

TABLE I
NUMERICAL VALUES OF $A/\mu(E_{ci})^2$ FOR TOROID ELECTRODE IN FREE SPACE

b/r	$A/\mu(E_{ci})^2$
40	5.77
60	6.17
80	6.46
100	6.69
125	6.91
150	7.09
175	7.24
200	7.38

which, substituting $r/b = x$, yields

$$\Delta V \leq \left[1 + G(x) + x\frac{dG}{dx}\right] \cdot \Delta r \cdot E_{ci} \tag{20}$$

substituting for ΔV and Δr from (17) and (18)

$$A \leq \left[1 + G(x) + x\frac{dG}{dx}\right] \mu E_{ci}^2. \tag{21}$$

Numerical values of the interesting quantity $A/\mu(E_{ci})^2$ for a wide range of b/r are given in Table I

A comparison of (8) for the spherical (point) electrode treated in [16] shows that for the same value of E_{ci}, the critical voltage rate that if exceeded would cause ultra-corona instability is approximately three times or higher for the toroid than for the sphere (point) electrode assumed to be in ultra-corona and confirms the superiority of the toroidal electrode for potential applications in lightning protection atop a tall structure.

Further examination of (21) shows that it constitutes a general formula which determines the critical rate of voltage rise for ultra-corona stability which applies for spherical, cylindrical as well as toroidal electrodes. Referring to (15), a spherical electrode corresponds to $G(r/b) = 1$, which when substituted in (21) yields a result identical to (8). For a cylindrical conductor, with $x = r/h$, $G(x) = -\ln(x/2)$, substituting in (21) results in an A value identical to (14).

B. Practical Ultra-Corona Electrodes

In the previous theoretical analysis, it was assumed that the electrode was in ultra-corona without demonstrating that this was actually the case for the geometries involved. As previously mentioned Uhlig has established that the elongated, longitudinal section formed between the two termini of a very thin wire (not points) comprises the ideal electrode for producing ultra-corona [7]. Since extremely thin wires are mechanically fragile, consideration should be given to stranding of the wires as well as the use of conducting fibers or filaments which can be bundled and woven into fabrics essentially made of thin fibers or wires. In his tests at Hydro-Quebec Research Institute (IREQ), Heroux [9] wrapped thin fibers, as well as tissues in the form of tapes with some stainless steel content, around power conductors which caused substantial improvement in radio interference and audible noise. As mentioned before, this improvement was achieved through generation of glow mode corona or production

of substantial rates of space charge at the expense of increased corona losses.

For potential lightning protection application, bundles of fibers or filaments or stranded wires or fabrics made from such fibers or wires, which in our case were made of 100% stainless steel were wrapped around grounded toroid electrodes to practically form a coil. The toroid electrode was also made of stainless steel. The stainless steel tape or tissue was glued at certain points to the stainless steel toroid surface to ensure durability. The dimensions of the toroid electrodes tested at the Hydro Quebec Research Institute (IREQ) for different applications had minor diameters of 1 cm, 2 cm, and 2.5 cm. The major diameters were 12 cm, 15, cm and 1 m, respectively. They were assembled as double toroids with distance between toroids of 3 cm, 5 cm, and 30 cm, respectively.

It is recognized that in potential lightning protection applications, the substantial space charge production in the glow mode and their associated corona losses will be of no major concern for the following reasons:

- a thin wire, fiber or fabric clad grounded toroid electrode atop a tall structure draws its current through the cloud generated ambient fields and is of relatively short duration and is not paid for by the user;
- the same applies if the thin wire, fiber, fabric clad conductor is used as a ground wire;
- if a thin wire, fiber, or fabric is wrapped around a power conductor, the effect of the resulting increase in corona losses should be limited by restricting this application to relatively short conductor lengths (e.g., river crossings or in and around substations).

To test the robustness of the 1m toroid electrodes, they were exposed to two years of outdoor weather in Montreal. This included two Canadian winters with atmospheric pollution, rain, snow, and ice. The electrodes were inspected regularly and did not show any signs of deterioration.

V. High Voltage Laboratory Tests

A. Test Setup

A schematic diagram of the test circuit, including a test object, is shown in Fig. 3. The test setup comprised a circular 6.1 m diameter aluminum mesh plate electrode suspended from the laboratory ceiling by insulating ropes 5 m above ground, serving as the high voltage electrode. The test object comprised a double toroid stainless steel electrode supported by a 10 cm diameter pole grounded through coaxial measuring shunts. The air gap was maintained at 1.5 m. The major diameter of the toroids was 1 m, the minor diameter was 2.5 cm and the distance between the individual toroids was 30 cm. Four objects were tested: one double toroid was left bare and served as reference, while three other electrodes were wrapped with varying quantities of:

- a $50\ \mu\mathrm{m}$ diameter stainless steel wire;
- a bundle of 275 filaments of a $12\ \mu\mathrm{m}$ stainless steel fiber;
- a woven fabric made of a bundle of filaments of a $12\ \mu\mathrm{m}$ stainless steel fiber.

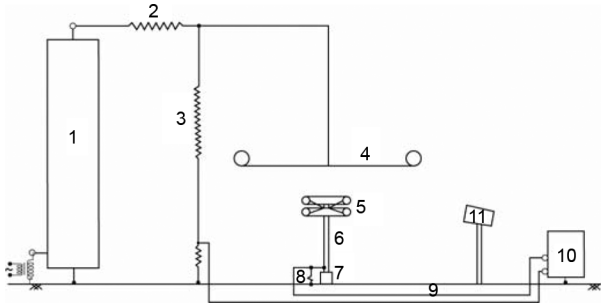

Fig. 3. Schematic diagram of the test circuit and test object. 1: HV cascade rectifier, 2: damping resistor, 3: direct voltage divider, 4: plane electrode, 5: double toroid test object, 6: steel pole, 7: insulator, 8: coaxial shunt, 9: coaxial measuring cables, 10: voltage and current measuring system, and 11: UV camera, video camera, acoustic microphone.

B. Test Technique

The high voltage plane electrode was energized from an HVDC 1.2 MV, 100 mA cascade and the polarity was negative. In each test the voltage was raised to 600 kV in approximately 45 s, maintained at the 600 kV voltage level for approximately 60 s and then raised gradually to breakdown. The following measurements were undertaken during each test:

- test voltage using a high ohmic voltage divider and a peak voltmeter;
- discharge current, where the voltage across the measuring noninductive shunt was monitored by:
  - a digital recording system having a sampling rate of 25 kHz and which retains the highest signal in 5 s intervals; the system was adequate to measure glow current component and associated charge;
  - a 100 MHz, 10 bit Nicolet digitizer to detect streamer current pulses;
  - a Tektronix oscilloscope model TDS5104B which allows treatment of measuring results to provide quantities such as statistical distribution of current pulses, integration of leakage current within a certain time interval, to display associated charge, etc.

The test object was also visually monitored during the test with:

- a UV camera to detect discharge activity;
- a video camera.

A directional microphone (sniffer) was also used to localize any audible noise source (streamers) from the test object or elsewhere on the high voltage connections.

The following quantities were considered of particular interest during tests on the different electrodes:

- corona inception voltage of the double toroid electrode as indicated by the start of discharge current flow $(\mathrm{sensitivity} \approx 10\ \mu\mathrm{A})$;
- variation of corona current mode and magnitude with voltage (time) during the test;
- quantity of generated space charge at different voltage levels;
- air gap breakdown voltage.

These tests were carried out under both dry conditions and with the double toroids electrodes thoroughly wetted with tap water.

TABLE II
TEST SERIES 1 CORONA INCEPTION RESULTS

Electrode No.	Cladding	U_{ci}, kV	
		Dry	Wet
1	Bare	435	239
2	Single 50μm Wire 1cm winding pitch	388	268
3	Woven Fabric 5cm tape, almost full surface coverage	155	150

It is noted that for a test voltage of 600 kV and a gap of 1.5 m, the mean voltage gradient of 400 kV/m corresponds to realistic fields at the top of a tall structure (Fig. 2).

In the second series of tests the different double toroid electrodes were suspended at a distance of 3.5 m above a $6\ \mathrm{m} \times 5\ \mathrm{m}$ conducting plane placed on the laboratory floor and connected to ground through a measuring shunt.

The test voltage was directly applied to the toroids and was normally raised in steps of approximately 50 kV and durations of approximately 2 minutes until a voltage level of 800 kV was reached. As expected this voltage was not sufficient to cause breakdown of the 3.5 m gap.

In this test series the current was measured at the ground terminal of the high voltage source and therefore includes the current of the high ohmic voltage divider. The current received by the ground plane was also measured

C. Test Results

In the first test series with the toroid below the energized plane, corona inception on all electrodes occurred during the ramp while the voltage is raised, as mentioned above, in 45 s to reach the 600 kV level (negative polarity). The corona inception results are shown in Table II for the three electrodes tested.

It is observed that under dry conditions, the corona inception voltage of the bare toroid is 2.8 times the corresponding value for the toroid with the 5 cm stainless steel woven fabric tape. The corona inception voltage of the toroid with the single $50\ \mu\mathrm{m}$ wire is also much higher than the corresponding value for the electrode with the 5 cm woven fabric tape. It is also noted that for the woven fabric clad electrode there is practically no difference between corona inception voltages under dry and wet electrode conditions. For the bare toroid on the other hand the inception voltage under wet electrode conditions is only 55% of the dry value, while the single $50\ \mu\mathrm{m}$ wire clad toroid the corresponding value is 69%.

In the second test series with the toroid suspended 3.5 m above ground, Table III, the corona inception voltage of the bare toroid is also three times the corresponding value for both the woven fabric clad electrode and the bundle of 275 filament clad electrode. Under wet electrode conditions the corona inception voltage of the bare toroid is 56% of the corresponding dry value. For both the woven fabric clad electrode and the bundle of 275 filament clad electrode, the dry and wet corona inception voltages are again identical.

TABLE III
TEST SERIES 2 CORONA INCEPTION RESULTS

Electrode No.	Cladding	U_{ci}, kV	
		Dry	Wet
1	Bare	450	250
2	Single 50μm Wire 1cm winding pitch	350	250
3	Woven Fabric 5cm tape, almost full surface coverage	150	150
4	Bundle of 275-12μm filaments Varying winding pitch Substantial surface coverage	150	150

TABLE IV
STREAMER CURRENT PULSE ACTIVITY OF DIFFERENT ELECTRODES IN THE FIRST TEST SERIES

No.	Cladding	Applied Voltage kV	Streamer Impulse Current Amplitude	
			Dry	Wet
1	Bare	600	166mA	42-52mA
2	Single 50μm Wire 1cm winding pitch	600	150-200mA	
		300		52mA
3	Woven Fabric 5cm tape, almost full surface coverage	600	Pulseless	Pulseless

Table IV summarizes the streamer current pulse amplitudes for electrodes number 1 and 2 at 600 kV under dry and wet electrode conditions. It is shown that for the bare electrode streamer impulse currents are reduced when the electrode is wet.

The performance of the toroid with a single $50\ \mu\mathrm{m}$ wire appeared to be not much different from the bare toroid. However it was observed from both current measurement and UV and video camera records that at the 600 kV level, under dry conditions, streamer activity on the toroid with the single $50\ \mu\mathrm{m}$ wire was intermittently completely suppressed. It was therefore suspected that the unsatisfactory performance was due to insufficient cladding due to the 1 cm winding pitch of a single wire which left too much exposed surface area of the toroid. This hypothesis was later confirmed by a separate test series reported below in which the voltage-current characteristics of different claddings on 12 cm diameter double toroids were performed.

The performance of the woven fabric clad electrode no. 3 was extremely satisfactory. At 600 kV there was no streamer activity (both UV and video camera) and no current impulses under both wet and dry electrode conditions. The pulseless glow current at 600 kV (corresponding to an electrode space potential of 420

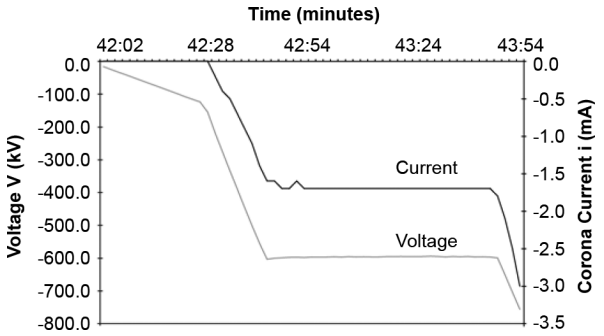

Fig. 4. Measured current voltage characteristics of the dry electrode.

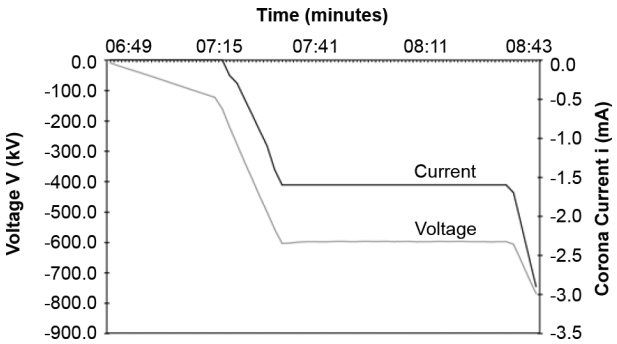

Fig. 5. Measured voltage current characteristics of the wet electrode.

TABLE V
SPARKOVER VOLTAGE OF 1.5 m GAP WITH DIFFERENT ELECTRODES IN FIRST TEST SERIES

No.	Cladding	Sparkover Voltage, kV		Sparkover Gradient, kV/m	
		Dry	Wet	Dry	Wet
1	Bare	677 –697	699	451 - 465	466
2	Single 50μm Wire 1cm winding pitch	709 –712	696- 747	473 - 475	464 - 498
3	Woven Fabric 5cm tape, almost full surface coverage	829 –840	803 - 810	553 - 560	535 - 540

kV) amounted to 1.7 mA, which lasted for 60 s, corresponding to a total charge of 100 mC as shown in Fig. 4 (dry) and Fig. 5 (wet electrode).

Table V shows results as the voltage was raised from 600 kV to a sparkover of the 1.5 m gap with the different electrodes. As is typical with dc, the results show little dispersion. There is also little difference between sparkover voltage with dry or wet electrodes.

There is a significant improvement in the sparkover voltage for the woven fabric clad electrode over the bare toroid electrode which can be attributed to the generation of streamer-free space charge, which reduced the electric field in the toroid vicinity but, of course, increased the field in the proximity of the plane

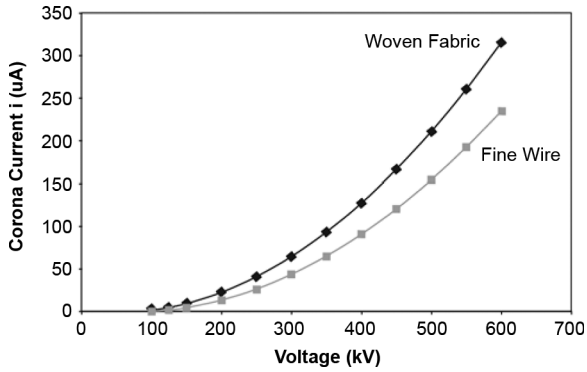

Fig. 6. Corona current-voltage characteristics of double toroids in 3 m gap.

electrode. The improvement in the sparkover gradient however is much less than that reported by Uhlig [7] for a simple thin wire-ground gap.

Fig. 6 shows the corona current-voltage characteristics of a 3.05 m gap with grounded double toroids with different claddings mounted below a 4 conductor bundle energized with negative dc voltage. The toroids had 12 cm major diameter and 1 cm minor diameter. One electrode was clad with stainless steel woven fabric made of 12 μm diameter filaments while the second was clad with closely wound single bare round wires of 40 μm diameter. The results show that the corona inception voltage of the two electrodes was quite close (around 100 kV). For the same voltage, the corona current of the fabric clad electrode was somewhat higher than the single wire clad electrode. With the conductor bundle at 600 kV (negative), the corona current from the woven fabric $(12\ \mu\mathrm{m})$ clad electrode amounted to $315\ \mu$A while that of the $40\ \mu$m wire clad electrode was $230\ \mu$A. In both cases the corona current was pulseless confirming the absence of streamers.

VI. GENERALIZATION OF CORONA CURRENT

For the practical case of an ultra-corona producing device atop a tall structure, corona current calculation by analytical methods can only be made under drastically simplified assumptions. This is bound to limit practical value of the results, since some factors will necessarily be missing from the analysis. Therefore dimensional analysis [23] will be applied to the problem in this section.

Consider an ultra-corona producing device atop a tall structure of height h above ground and a structure radius a. Consider an ambient ground field E_g which will be intensified due to the structure geometry to produce a field E_t at the location of the ultra-corona device. In general

$$\frac{E_t}{E_g} = f\left(\frac{h}{a}\right) \tag{22}$$

which can be determined either analytically or by charge simulation. Let the space potential at the device position be V_s and let the corona inception space potential of the ultra-corona producing device be V_{ci}.

Consider that the ultra-corona electrode is a double toroid of major radius b and minor radius r. Let us assume that the space charge removal from the electrode vicinity is mainly caused by

TABLE VI
COMPARISON OF FORMULA (27) WITH MEASURED CORONA CURRENT FOR DIFFERENT TOROIDAL ELECTRODES

b/r	V_s, kV	V_{ci}, kV	E_t, kV/m	i, mA	
				Formula (27)	Measured
40	420	105	400	1.65	1.70
40	400	150	114	0.37	0.36
12	226	37.7	200	0.33	0.34

the increased positive ion speed at the intensified electric field Et, rather than the relatively slow expansion of the space charge cloud due to the time rate of rise of space potential considered in [16]. The major parameters influencing the corona current i are: the excess space potential $V_s - V_{ci}$, the electric field E_t in which the device is immersed, the dimensions b and r of the device, the mobility μ of positive ions and the space permittivity ε_o. These variables will, in general, be related by a function of the form

$$F(i,\ V_s - V_{ci},\ E_t,\ b,\ r,\ \mu,\ \varepsilon_o) = 0. \tag{23}$$

Dimensional analysis results in two independent dimensionless variables so that

$$F\left[\frac{i}{\varepsilon_o \mu E_t (V_s - V_{ci})},\ \frac{b}{r}\right] = 0. \tag{24}$$

The corona current can therefore be expressed as

$$i = f\left(\frac{b}{r}\right) \cdot \varepsilon_o \mu E_t (V_s - V_{ci}). \tag{25}$$

From laboratory tests on air gaps with double toroid electrodes having b/r of 7.5, 12, and 40, an approximate empirical expression of $f(b/r)$ was obtained

$$f\left(\frac{b}{r}\right) \approx \text{const.} \sqrt[3]{\frac{b}{r}}. \tag{26}$$

The constant in (26) depends on the electrode surface conditions and for the woven fabric clad electrode amounts to approximately 2.88. Substituting (26) into (25) we get

$$i = 2.88 \cdot \sqrt[3]{\frac{b}{r}} \varepsilon_o \mu E_t (V_s - V_{ci}). \tag{27}$$

Table VI serves as a numerical check for (27) in which calculations of corona currents for different woven fabric clad electrodes are compared with the measured values.

Voltages in the first and third tests reported refer to space potentials of the grounded electrodes

For these laboratory gaps E_t is taken as the mean voltage gradient across the air gap [24].

Fig. 7 shows computed variation of the corona current from an ultra-corona device $(b/r = 40)$ installed on a 2 m pole atop a semi-ellipsoid structure on flat ground of height 70 m and $h/a = 50$, with ambient ground field. It is shown that a current of 1.2 mA is reached at $E_g = 20\ \text{kV/m}$. It may be noted that

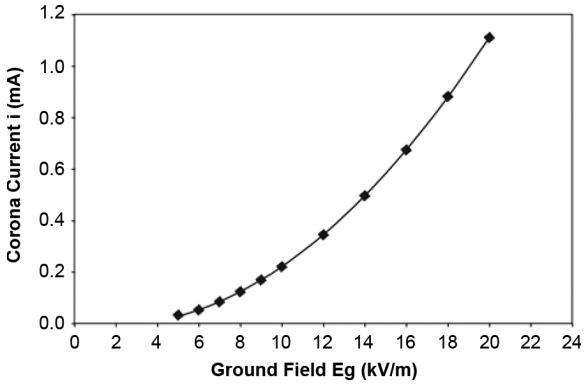

Fig. 7. Corona current from ultra-corona device on 70 m structure $h/a = 50$.

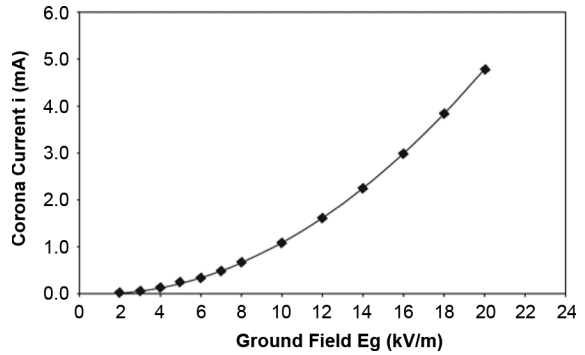

Fig. 8. Corona current from ultra-corona device on 200 m structure, $h/a = 100$.

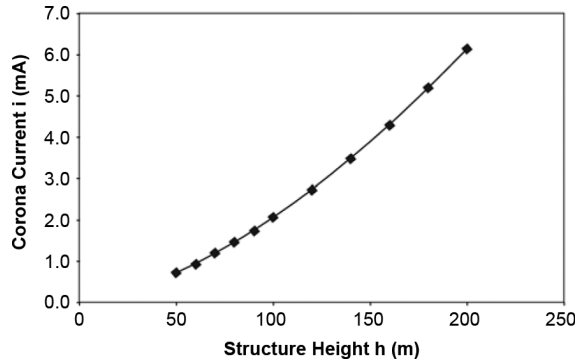

Fig. 9. Corona current variation with structure height, $a = 1$ m, $Eg = 20\ \text{kV/m}$.

the highest corona current level reported by Berger on his 70 m tower [25] reached 3 mA.

Fig. 8 shows similar computed results for the same ultra-corona device atop a 200 m semi-ellipsoid structure, with $h/a = 100$. Here, the current reaches 3 mA at the lower ground field of 16 kV/m.

Fig. 9 shows computed variation of the current from the ultra-corona device with semi-ellipsoid structure heights in the range of 50–200 m for $a = 1$ m, $E_g = 20\ \text{kV/m}$. The corona current is as low as 716 μA for the 50 m structure but reaches 6.14 mA for the 200 m structure, at such value of the ground field.

In (27) it is noted that the term μE_t determines the positive ion speed v_i by which positive ions are removed due to

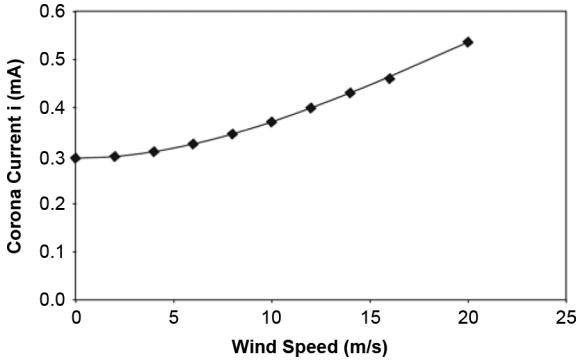

Fig. 10. Effect of wind speed on corona current, $h = 200$ m, $h/a = 200$, $Eg = 5$ kV/m.

the ambient field E_t at the ultra-corona device location. If ions are also displaced horizontally due to wind speed v_W, the term μE_t should according to Large and Pierce [21] be replaced by $\sqrt{(\mu E_t)^2 + v_w^2}$, so that (27) becomes

$$i = 2.88 \cdot \sqrt[3]{\frac{b}{r}} \varepsilon_o \sqrt{(\mu E_t)^2 + v_w^2} \cdot (V_s - V_{ci}). \qquad (28)$$

Fig. 10 shows the effect of wind speed on corona current, for a 200 m structure with $h/a = 200$ at an ambient ground field of 5 kV/m. The wind speed was varied in the range $0 - 20$ m/s. At such relatively low ground fields, we found a substantial effect of wind speed on corona current, otherwise with high field intensification at the tower top the component μE_t in (28) dominates.

VII. Future Work

Recognizing the importance of field tests to assess the performance of the ultra-corona device [26] presented before, some devices have been installed on 120 m river crossing towers. The device current and the structure current are being separately monitored by magnetic cards. Results from this test program will be reported as they accumulate. Finally, this paper deals exclusively with technical performance of ultra-corona devices. Specific future applications may involve cost-benefit analysis in comparison with existing technologies.

VIII. Conclusions

Based on theoretical analysis and experimental results, the following conclusions have been reached.

1) Electric field intensification at a structure top due to the high ratio of structure height to diameter will have serious effects on the streamer growth.
2) The prerequisites for the beneficial effects of space charge on leader inception are therefore:
   - strict streamer-free corona mode (ultra-corona) over a wide ambient field range;
   - stability of the ultra corona under rapid variation of the ambient field.
3) It has been shown that with view of the stability of ultra-corona a cylindrical conductor or toroidal electrode have far superior performance compared to a sphere (point) electrode.
4) The aforementioned conclusions contest the practical application of point electrodes for space charge-based lightning protection since they are prone to streamer formation.
5) A novel lightning protection electrode to be mounted on tall structures has been presented which is characterized by the following unique features:
   - a very thin conductor-based cladding which provides an ultra-corona producing element for streamer inhibition;
   - a toroidal electrode shape which contributes to enhancement of ultra-corona stability;
   - the very thin conductor would also boost the critical rate of voltage (space potential) rise.
6) High voltage laboratory tests on a grounded pole-mounted ultra-corona generating toroidal electrode under a large plane electrode energized with a negative direct voltage with electrical and optical measuring techniques demonstrated:
   - a much lower corona inception voltage compared with a bare electrode of the same dimensions;
   - the absence of streamers over a wide voltage range right up to air gap breakdown
   - production of corona currents at a space potential of 420 kV as high as 1.7 mA corresponding to a charge of 17 mC in a 10 s duration;
   - a complete lack of sensitivity to the presence of water drops on the electrode surface;
   - improved air gap breakdown voltage.
7) A new formula based upon dimensional analysis was deduced relating corona current from the ultra-corona device atop a tall structure to ambient ground field, structure height, field intensification at the structure top, dimensions of the device and wind speed.
8) It was shown that above corona inception, the current from the ultra-corona device atop a tall structure:
   - increases almost quadratically with the ground field, for a given structure height;
   - increases less than quadratically with structure height, for a given ambient ground field.
9) For tall structures with substantial field intensification at the top, the effect of wind speed on corona current is more significant for lower values of the ambient ground field.

References

[1] V. A. Rakov and M. A. Uman, "Lightning physics and effects," in *Downward Negative Lightning Discharges to Ground*. Cambridge, U.K.: Cambridge Univ. Press, 2003, ch. 4, pp. 108–213.
[2] E.M. Bazelyan and Y. P. Raizer, *Lightning Physics and Lightning Protection*. London, U.K.: Inst. Physics Publishing, 2000, p. 21.
[3] B. Glushakow, "Effective lightning protection for wind turbine generators," *IEEE Trans. Energy Convers.*, vol. 22, no. 1, pp. 214–222, Mar. 2007.
[4] C. B. Moore, W. Rison, J. Mathis, and G. Aulich, "Lightning rod improvements," *J. Appl. Meteorol.*, vol. 39, pp. 593–609, 2000.
[5] F. A. M. Rizk, "Switching impulse strength of air insulation: Leader inception criterion," *IEEE Trans. Power Del.*, vol. 4, no. 4, pp. 2187–2195, Oct. 1989.
[6] F. A. M. Rizk, "Modeling of transmission line exposure to direct lightning strokes," *IEEE Trans. Power Del.*, vol. 5, no. 4, pp. 1983–1997, Nov. 1990.

[7] C. A. E. Uhlig, "The ultra corona discharge, a new phenomenon occurring on thin wires," in *High Voltage Symposium, National Research Council of Canada*, Ottawa, ON, Canada, 1956.
[8] V. I. Popkov, "Some special features of corona on high voltage DC transmission lines," in *Gas Discharges and the Electricity Supply Industry Paper no. 38*. London, U.K.: Butterworths, 1962, pp. 225–237.
[9] P. Heroux, P. S. Maruvada, and N. G. Trinh, "High voltage AC transmission lines: Reduction of corona under foul weather," *IEEE Trans. Power App. Syst.*, vol. PAS-101, no. 9, pp. 3009–3017, Sep. 1982.
[10] N. G. Trinh and J. B. Jordan, "Modes of corona discharges in air," *IEEE Trans. Power App. Syst.*, vol. PAS-87, no. 5, pp. 1207–1215, May 1968.
[11] R. H. Golde, "The lightning conductor," in *Lightning*. London, U.K.: Academic Press, 1977, vol. 2, ch. 17, pp. 545–576.
[12] R. B. Carpenter and R. L. Auer, "Lightning and surge protection of substations," *IEEE Trans. Ind. Appl.*, vol. 31, no. 1, pp. 162–174, Jan./Feb. 1995.
[13] M. A. Uman and V. A. Rakov, *Critical Review of Nonconventional Approaches to Lightning Protection*. Boston, MA: Bull. Amer. Meteorol. Soc., 2002, pp. 1809–1820.
[14] N. L. Aleksandrov, E. M. Bazelyan, and Y. P. Raizer, "The effect of corona discharge on lightning attachment," *Plasma Phys. Rep.*, vol. 31, no. 1, pp. 75–91, 2005.
[15] A. M. Mousa, "The application of lightning elimination devices to substations and power lines," *IEEE Trans. Power Del.*, vol. 13, no. 4, pp. 1120–1127, Oct. 1997.
[16] N. L. Aleksandrov, E. M. Bazelyan, R. B. Carpenter, M. M. Drabkin, and Y. P. Raizer, "The effect of coronae on leader initiation and development under thunderstorm conditions and in long air Gaps," *J. Phys. D.:Appl. Phys.*, vol. 34, pp. 3356–3266, 2001.
[17] N. L. Aleksandrov, E. M. Bazelyan, M. M. Drabkin, R. B. Carpenter, and Y. P. Raizer, "Corona discharge at the tip of a tall object in the electric field of a thundercloud," *Plasma Phys. Rep.*, vol. 28, no. 11, pp. 953–964, 2002.
[18] E. M. Bazelyan, N. L. Aleksandrov, F. D'Alessandro, and Y. P. Raizer, "Numerical simulation of thunderstorm induced processes near lightning rods installed on grounded structures," in *Proc. 28th Int. Conf. Lightning Protection*, 2006, pp. 564–569.
[19] F. J. W. Whipple and F. J. Scrace, "Point discharge in the electric field of the earth," in *Geophys. Memoirs*. London, U.K.: Meteorol. Office, No. 68, 1936, pp. 1–20.
[20] R. Davis and W. G. Strandring, "Discharge current associated with kite balloons," *Proc. Roy. Soc. London, Ser. A*, vol. 191, no. 1026, pp. 304–322, Nov. 1947.
[21] M. I. Large and E. T. Pierce, "The dependence of point-discharge currents on wind as examined by a new experimental approach," *J. Atmosph. Terrestrial Phys.*, vol. 10, pp. 251–257, 1957.
[22] F. A. M. Rizk, "A model for switching impulse strength of large air gaps," *IEEE Trans. Power Del.*, vol. 4, no. 1, pp. 596–606, Jan. 1989.
[23] H. L. Langhaar, *Dimensional Analysis and Theory of Models*. New York: Wiley, 1951.
[24] G. F. Ferreira, O. N. Oliviera, and J. A. Giacometti, "Point-to-Plane corona: Current voltage characteristics for positive and negative polarity with evidence of an electronic component," *J. Appl. Phys.*, vol. 59, no. 9, pp. 3045–3049, May 1986.
[25] K. Berger, "The earth flash," in *Lightning*, R. H. Golde, Ed. London, U.K.: Academic, 1977, vol. 1, p. 169.
[26] "Lightning protection device: Wet/dry glow based streamer inhibitor," U.S. Patent 7 468 879.

Farouk A. M. Rizk (LF'09), photograph and biography not available at the time of publication.